A single-site reactive transport model of Cs^+ for the *in situ* diffusion and retention (DR) experiment

Shuping Yi[1,2], Javier Samper[2], Acacia Naves[2] & Josep M. Soler[3]

1. Electric Power Design Institute, China Energy Engineering Group Co., LTD., 510663, Guangzhou, China. yishuping@gedi.com.cn
2. ETS ICCP Universidad de A Coruña. Campus de Elviña, ES-15192, A Coruña, Spain
Javier Samper: jsamper@udc.es; Acacia Naves: anaves@udc.es
3. Josep M. Soler. IDAEA-CSIC, Barcelona. Spain. josep.soler@idaea.csic.es

Abstract

In situ diffusion experiments are performed in underground research laboratories for understanding and quantifying radionuclide diffusion from underground radioactive waste repositories. The *in situ* diffusion and retention, DR, experiment was performed at the Mont Terri underground research laboratory, Switzerland, to characterize the diffusion and retention parameters of the Opalinus clay. Several tracers were injected instantaneously in the circulating artificial water and then were allowed to diffuse into the clay rock through two porous packed-off sections of a borehole drilled normal to the bedding of the clay formation. This paper presents a single-site multicomponent reactive transport model of Cs^+, a tracer used in the DR experiment which sorbs onto Opalinus clay via cation exchange. The reactive transport model accounts for the diffusive reactive transport of 11 primary species and 22 aqueous complexes and the water-rock interactions for 5 cation exchange and 3 mineral dissolution/precipitation reactions. Most of the solutes except for Cs^+ diffuse from the Opalinus clay formation into the injection interval because the concentrations in the initial Opalinus clay pore water are larger than those of the initial water in the circulation system. Calcite dissolves near the borehole while dolomite precipitates. Dissolved Cs^+ sorbs by exchanging with Ca^{2+} in the exchange complex. The computed dilution curve of Cs^+ in the circulating fluid is most sensitive to the effective diffusion, D_e, of the filter, the selectivity coefficient of Na^+ to Cs^+, $K_{Na\text{-}Cs}$ and the D_e of the borehole disturbed zone. The apparent distribution coefficient of Cs^+, K_d^a, in the formation varies in space and time from 100 to 165

L/kg due to the temporal changes in the water chemistry in the formation. The results of a sensitivity run in which the initial chemical composition of the Opalinus pore water is the same as the initial chemical composition of the water in the circulation system show that the changes in K_d^a are negligible. The dilution curve of Cs^+ computed with the reactive transport model coincides with that obtained with the K_d model. The tracer concentrations along the overcoring profiles computed with the K_d model, however, differ significantly from those computed with the reactive transport model. Therefore, a reactive transport model is needed for the appropriate interpretation of the Cs^+ overcoring data from the DR diffusion experiment.

Keywords: Radionuclide diffusion, reactive transport model, cation exchange, Cs^+, in situ diffusion and retention test, Opalinus Clay, Switzerland

1. Introduction

Argillaceous formations are being considered as potential host rocks for the deep geological disposal of radioactive waste. The performance assessment of such host rocks as geological barriers requires understanding and quantifying radionuclide diffusion and sorption from laboratory experiments, field studies and numerical modeling. Radionuclide diffusion and sorption are key processes for the safety of underground radioactive waste repositories. Selecting the appropriate sorption conceptual model is at least as important as estimating the optimal sorption parameters. Dai et al. (2012) used inverse modeling to identify neptunium and uranium sorption processes. Dai et al. (2009) studied the scale dependence of sorption coefficients in fractured rock caused by physical and chemical heterogeneities.

Various experimental programs are being carried out at the Mont Terri Underground Research Laboratory (URL) in Switzerland to study the feasibility of the Opalinus Clay formation to host a radioactive waste repository. Such programs aim at analyzing the hydrogeological, geochemical and rock mechanical properties of the argillaceous formation, evaluating the changes of these properties induced by the excavation of galleries and improving

the investigation techniques. The Opalinus Clay formation is an overconsolidated shale formation with an extremely low hydraulic conductivity. No natural water inflows or wet areas were observed in the URL galleries. Molecular diffusion is expected to be the dominant transport mechanism. In situ diffusion experiments were performed in URL's to quantify tracer diffusion and sorption parameters and investigate scale effects (Palut et al. 2003; Tevissen et al. 2004; Yllera et al. 2004; Van Loon et al. 2004; Wersin et al. 2004 2008; Samper et al. 2006a). The *in situ* diffusion and retention (DR) experiment was performed at the Mont Terri URL in the Opalinus (OPA) clay. It was designed based on previous *in situ* diffusion experiments such as the DI-A (Wersin *et al*. 2004; Van Loon *et al*. 2004), DI-A2 (Wersin *et al*. 2008; Soler et al. 2013) and DI-B (Yllera et al. 2004; Samper *et al.* 2006a; Soler et al. 2008) in the OPA clay and the DIR experiments in the Callovo-Oxfordian clay (Dewonck, 2007; Samper *et al.* 2008a). The DR experiment was performed to: (i) obtain diffusion and retention data for moderately and strongly sorbing tracers, (ii) improve the estimation of diffusion anisotropy and (iii) quantify the effects of the borehole disturbed zone for non-reactive tracers. The diffusion test took place in two packed off sections of a borehole in the DR niche at the Mont Terri URL (Gimmi et al. 2014). The two packed off borehole sections were connected to the surface equipment where the artificial pore water was contained in a reservoir tank of 20 L. The artificial pore water was continually pumped through the connecting tubes to ensure tracer mixing between the tank and the downhole water. The tracers (I, Br, ^{22}Na, ^{85}Sr, Cs, ^{137}Cs, ^{133}Ba, ^{60}Co ^{152}Eu, and ^{75}Se) were injected as a pulse to the circulating fluid and allowed to diffuse into the clay rock through a porous Teflon membrane in the packed off sections of the borehole. The fading tracer concentrations were monitored with a gamma spectrometer and by chemical analyses. At the end of the experiment the downhole equipment was extracted from the borehole, which was then overcored. Tracer diffusion profiles were analyzed from the overcored rock material (Gimmi et al. 2014). Figure 1 shows the location of the Mont Terri URL and the situation of the DR borehole.

Cs^+ is one of the tracers used in the DR experiment. Cs^+ sorption onto clay occurs mainly

via cation exchange. This reaction is fast and can be treated at local chemical equilibrium (Tsai et al. 2001; García-Gutiérrez et al. 2001; Murali and Mathur, 2002; Shahwan and Erten, 2002; Khan, 2003; Atun and Kilislioglu, 2003; Jan et al. 2006; Montavon et al. 2006). Cs^+ sorption depends on the concentration of dissolved Cs^+, the concentrations of other dissolved cations, the pH, the ionic strength, the solid-to-liquid ratio and the mineralogical composition of the clay (Gutiérrez and Fuentes 1996; Tsai et al. 2001; Atun and Bodur 2002; Tertre et al, 2005; Klika et al. 2007). Samper et al. (2010b) performed long-term simulations of Cs^+ sorption in the bentonite barrier of a radioactive waste repository and found that the sorption of Cs^+ is inversely correlated with the ionic strength for concentrations of dissolved $Cs^+ < 10^{-5}$ mol/L.

Lauber et al. (2000) performed batch sorption experiments on OPA clay samples and synthetic OPA clay pore water and derived nonlinear isotherms. Bradbury and Baeyens (2000) constructed a generalized 3-site cation exchange sorption model of Cs^+ for pure illite, which covers a wide range of Cs^+ concentrations from 10^{-8} to 10^{-3} mol /L. Previous studies of tracer migration through the Opalinus (OPA) clay were based on the use of the distribution coefficient, K_d (Wersin et al. 2004; Van Loon et al. 2004; Samper et al. 2010). Jakob et al. (2009) compared the performance of a nonlinear isotherm model with a multicomponent reactive transport model (MRTM) of Cs^+ for a through-diffusion laboratory experiment. They concluded that Cs^+ sorption in such diffusion experiments cannot be addressed by a nonlinear isotherm formalism. A reasonable analysis of such tracer diffusion experiments requires the use of a MRTM to account for the transport (diffusion) and sorption of the main cations and the entire water chemistry of the system. Soler et al. (2013) presented a multisite MRTM model of Cs^+ for the DI-A2 experiment. The interpretation of this experiment with a K_d model leads to discrepancies between the Cs^+ sorption parameters derived from *in situ* and batch sorption experiments. They found that such discrepancies are overcome when the *in situ* test is interpreted with a MRTM.

Here we present a single-site MRTM to simulate the transport of Cs^+ through the OPA clay in the DR experiment. The paper starts by presenting the reactive transport model. Then,

model results are presented. The paper ends with a discussion of the results and the main conclusions.

2. Reactive transport model

2.1. Reactive transport

Solute transport in low-permeability formations takes place by molecular diffusion. If all the aqueous species have the same diffusion coefficient, the diffusive-reactive transport equations can be written in terms of total dissolved component concentrations, C_k, (Yeh, 2000):

$$\nabla \cdot (\phi \mathrm{D} \nabla \mathrm{C_k}) + \phi \mathrm{R_k} = \phi \frac{\partial \mathrm{C_k}}{\partial \mathrm{t}} \qquad \mathrm{k} = 1, 2, ..., \mathrm{N_c} \tag{1}$$

where **D** is the diffusion tensor, ϕ is the porosity, k refers to the chemical component from 1 to N_c, and R_k is the chemical sink/source term, which includes all the chemical interactions of the *k-th* component with the solid species (Xu et al. 1999). Geochemical reactions include: 1) Homogeneous reactions which occur in the liquid phase, such as aqueous complexation, acid-base and redox reactions and 2) Heterogeneous reactions which involve the exchange of mass between the liquid and the solid and the gaseous phases, and include mineral precipitation/dissolution, surface complexation, cation exchange and gas dissolution/exsolution.

The total dissolved concentration of a given component, C_k, can be written as a function of the concentrations of the N_C primary species, c_i, and the N_x concentrations of secondary species, x_j, according to (Xu *et al*. 1999):

$$C_k = c_k + \sum_{j=1}^{N_x} \nu_{jk} x_j = c_k + \sum_{j=1}^{N_x} \nu_{jk} \left(K_j^{-1} \gamma_j^{-1} \prod_{i=1}^{N_c} c_j^{\nu_{ji}} \gamma^{\nu_{ji}} \right) \tag{2}$$

where K_j is the equilibrium constant which depends on the pressure and temperature of the system; γ are the activity coefficients, and ν_{ij} is the stoichiometric coefficient of the *i-th*

primary species in the *j-th* aqueous complex.

Dissolution-precipitation reactions at chemical equilibrium can be described by the Law of Mass Action, which states that (Xu *et al*. 1999):

$$X_m \lambda_m K_m = \prod_{i=1}^{N_c} c_i^{\nu_{mi}^p} \gamma_i^{\nu_{mi}^p} \tag{3}$$

where X_m is the molar fraction of the m-th solid phase; λ_m is the thermodynamic activity coefficient (X_m and λ_m are taken equal to one for pure phases); ν_{mi}^p is the stoichiometric coefficient in the dissolution reaction of the *m-th* solid phase; and K_m is the corresponding equilibrium constant.

2.2 Transport model

The interpretation of *in situ* diffusion experiments is complicated by several non-ideal effects caused by the presence of a sintered filter, a gap between the filter and the borehole wall and a borehole disturbed zone (BDZ) which is assumed to have a porosity larger than that of the intact rock (Figure 2).

Symmetry with respect to the borehole axis allows the use of a 2D axi-symmetric model for modelling the DR experiment. Actually, Cs^+ migration can be modelled accurately with a 1D axisymmetric mesh because the radial penetration of the tracer front into the clay formation is smaller than the length of the injection interval (Samper et al. 2010a). Therefore, a 1D axi-symmetric grid of a unit vertical thickness was used to model the diffusive-reactive transport of Cs^+ from the injection interval into the OPA clay pore water in the *in situ* DR experiment.

The model domain consists of the following five material zones with a total radial extent of 1.8 m: the injection interval (0.5 mm), the filter (3 mm), the gap (2 mm), the BDZ (20 mm) and the undisturbed clay. The model domain was discretized using a 1D grid with 86 nodes. The grid has one node in the injection interval, 4 nodes in the filter, 3 in the gap, 22 in the BDZ and 56 in the undisturbed clay. All the primary and secondary aqueous species are assumed to

have the same transport parameters (effective diffusion and porosity) in each material zone. The parameters of the undisturbed clay were derived from Gimmi (2006). The D_e of the gap and the BDZ were computed from those of the undisturbed clay by using Archie´s law with an exponent of 1.33. The D_e of the filter was measured by van Loon and Glaus (2008) and is equal to 10% of the value in free water. The transport parameters are listed in Table 1.

A time domain of 1115 days was considered in the model. Temperature was assumed constant and equal to 25℃.

2.3. Geochemical model

The MRTM accounts for aqueous complexation, acid-base, mineral dissolution/precipitation and cation exchange reactions. The chemical system is defined in terms of the following primary species: H_2O, H^+, Ca^{2+}, Mg^{2+}, Na^+, K^+, Sr^{2+}, Cl^-, SO_4^{2-}, HCO_3^- and Cs^+. The relevant aqueous complexes were identified from speciation runs performed with EQ3/6 (Wolery 1992). The Opalinus clay pore water was assumed to be at local chemical equilibrium with respect to the following mineral phases: calcite, dolomite, and gypsum. The equilibrium constants for aqueous complexes and mineral phases were taken from the EQ3/6 data base (Wolery 1992). Cation exchange was modelled with a single type of cation exchange sites using the Gaines-Thomas convention (Gaines and Thomas, 1953). The selectivity coefficients for cation exchange reactions were taken from Pearson et al. (2003) except for the selectivity coefficient of Cs^+ to Na^+ (dimensionless), $K_{Na\text{-}Cs}$, which was estimated from the following expression (Appelo and Postma, 1993):

$$\mathrm{K_{Cs-Na}} = \frac{[\mathrm{Na^+}]}{\beta_{\mathrm{Na}}} \frac{100}{\mathrm{CEC}} \mathrm{K_d} \tag{4}$$

where K_d is the distribution coefficient (L/kg), CEC is the cation exchange capacity (meq/100g), β_{Na} is the equivalent fraction of exchanged Na^+ and $[Na^+]$ is the activity of dissolved Na^+ (mol/L). A K_d value of 157 L/kg was adopted based on available Cs^+ sorption

data on Opalinus clay for a Cs^+ concentration within the range 10^{-6} to 10^{-5} mol/L (Lauber et al. 2000). The resulting selectivity coefficient $K_{Na\text{-}Cs}$ is equal to $4.76 \cdot 10^{-4}$. The equilibrium constants for aqueous complexes, minerals and the selectivity coefficients for cation exchange reactions are listed in Table 2.

The initial chemical composition of the OPA pore water was taken from values reported for the OPA clay formation from previous studies (Jakob et al. 2009; Van Loon et al. 2009). The water in the circulation system is a synthetic water which has a chemical composition close to the average chemical composition of the OPA pore water. The composition of the water in the circulation was established during the design of the experiment (Gimmi *et al.* 2014). The initial concentrations of the chemical species in the OPA clay pore water are larger than those of the water in the circulation system (Table 3). It was assumed that the initial chemical composition in the pore water in the filter and the gap was equal to the initial chemical composition of the water in the circulation system.

The initial concentration of Cs^+ is equal to zero everywhere in the model domain. A pulse of Cs^+ was added to the injection interval after 35 days of circulation of the water in the injection system. The concentration of Cs^+ in the injection interval at t = 25 days is equal to $1.814 \cdot 10^{-4}$ mol/L.

The initial volume fractions of the minerals and the cation exchange capacity (CEC) of the OPA clay were taken from Pearson et al. (2003). The initial volume fractions of the minerals are 0.28, 0.02 and 0 for calcite, dolomite and gypsum, respectively. Other minerals of the OPA clay at the DR site include: clay minerals (60 to 65 wt.%), quartz (18.5 wt.%), siderite (2 wt.%), K-feldspars (2 wt.%) and albite (2 wt.%) (Gimmi *et al.* 2014). The CEC is equal to 11.68 meq/100g.

2.4 Computer code

The DR experiment was simulated with CORE^{2D}V4, a 2-D Galerkin finite element

multicomponent reactive transport code which solves for groundwater flow, heat transport and multicomponent reactive solute transport in saturated/unsaturated steady or transient groundwater flow under general boundary conditions (Samper et al. 2009; Samper et al. 2011). This code has been extensively used to model aquifer flow and solute transport in aquifers (Dai and Samper 2006), *in situ* diffusion experiments in clay formations (Yllera et al. 2004; Samper et al. 2006a; Samper et al. 2008a; Soler et al. 2008; Samper et al. 2010a; Naves et al. 2012; Yi et al. 2012), laboratory diffusion and retention experiments (Samper et al. 2006b), including the CERBERUS Experiment in the Boom clay (Zhang et al. 2006) and the Redox Zone Experiment in a fracture zone of the Äspö site (Molinero et al. 2004; Molinero and Samper, 2006). It has been used also to evaluate the geochemical evolution of radioactive waste repositories in clay (Yang et al. 2008) and granite (Yang et al. 2007), to model the transport of corrosion products and their geochemical interactions with bentonite (Samper et al. 2008b; Lu et al. 2011) and to study cation exchange and reactive transport in stochastically-heterogeneous aquifers (Samper and Yang, 2006)

3. Model results

3.1. Reactive transport model

The initial concentrations in the OPA pore water are larger than those of the water in the circulation system. Therefore, solutes diffuse from the clay formation into the injection interval. The computed concentrations of most of the chemical species in the test interval increase with time except for Cs^+.

Figure 3 shows the time evolution of the concentrations of exchanged cations at a point located within the BDZ at r = 0.48 m. One can see that the concentration of exchanged Ca^{2+} and Na^+ decrease from the beginning of the experiment, while those of exchanged Sr^{2+}, Cs^+ and K^+ increase. The concentration of exchanged Cs^+ rises rapidly at about 50 days and reaches a maximum after 400 days. The patterns of exchanged concentrations at other locations are

similar. The time at which the concentration of Cs^+ starts to rise grows with the radial distance.

The concentrations of exchanged Cs^+ near the injection interval increases mainly at the expense of the decrease of the concentration of exchanged Ca^{2+} (Figure 3). Therefore, Ca^{2+} is the cation that exchanges with Cs^+. Sorption of Cs^+ takes place mainly for $r < 0.09$ m after 1115 days (Figure 4).

Calcite precipitates and dolomite dissolves at $t = 0$ because the estimated initial OPA pore water is not exactly at equilibrium with these two minerals. After equilibration with calcite and dolomite, the pH decreases from 7.6 to 7.22, the concentration of Ca^{2+} decreases and that of Mg^{2+} increases slightly (Table 3). Once equilibrated, the trends of the minerals depend on the differences in the concentrations of the initial OPA pore water and the boundary synthetic water. The Ca^{2+} and Mg^{2+} concentrations in the initial OPA clay pore water are larger than those of the initial water in the circulation system. Therefore, Ca^{2+} and Mg^{2+} diffuse from the OPA clay formation into the injection interval. Since the contrast in the concentration of Ca^{2+} in the OPA clay water and in the initial water in the circulation system is larger than that of the concentration of Mg^{2+}, calcite dissolves to compensate for the lowering of the concentration of Ca^{2+}. Calcite dissolution increases the pH and the concentration of bicarbonate, which trigger the precipitation of dolomite. The rates of mineral dissolution/precipitation increase slowly with time (Figure 5). Gypsum does not precipitate because the sulfate concentration of the synthetic water in the circulation system is smaller than the initial sulfate concentration in the OPA pore water.

3.2. Sensitivity analysis

Parameter estimation errors are related to the sensitivities of concentrations to changes in parameters. Therefore, a detailed sensitivity analysis was performed to evaluate parameter uncertainties. The dilution curve of Cs^+ was computed first for a set of reference parameters. Sensitivity runs with these reference parameters were performed by changing one-at-a-time the

relevant parameters within prescribed ranges.

The results of the sensitivity runs show that the computed dilution curves of Cs^+ are sensitive to the changes in the effective diffusion, D_e, of the filter, the D_e of the BDZ and the selectivity coefficient of $K_{Na\text{-}Cs}$ (Figure 6), while they are not sensitive to the changes in the D_e of the gap and the undisturbed clay (not shown here). The computed dilution curves of Cs^+ lack sensitivity to the changes in the porosity of the filter, the gap, the BDZ and the undisturbed clay.

The sensitivities of Cs^+ concentrations to changes in parameters vary with time as reported by Samper et al. (2010a). The changes in D_e of the filter affect the dilution curve from the beginning of the experiment. The sensitivity is largest at about 200-300 days. Both early and late time data are less sensitive to changes in D_e of the filter than the intermediate times (Figure 6). The concentration of Cs^+ at the injection interval at early times is not sensitive to the changes in the D_e of the BDZ and the selectivity coefficient of $K_{Na\text{-}Cs}$. However, it is sensitive at later times (Figure 6). These results are similar to those reported by Samper et al. (2008a) for the DIR experiments performed in the Callovo–Oxfordian clay.

3.3. Charge balance errors

The computed aqueous solutions should remain neutral when the initial and the boundary waters are electrically neutral because reactive transport models usually preserve the charge balance (Dai et al, 2006). The initial waters in the model of the DR experiment are not fully neutral. Therefore, one should check the charge balance errors. The relative errors of charge balance have been calculated at the end of the simulation at radial distances equal to 0.048, 0.1, 0.5 and 1.0 m. They are listed in Table 4. The largest charge balance errors are smaller than 4% and occur near the injection interval where most of the geochemical reactions take place. The errors decrease with radial distance.

3.4 Apparent K_d^a of Cs^+

The apparent distribution coefficient of Cs^+, K_d^a, was calculated from the output results of the reactive transport model with the following equation (Samper et al. 2010b):

$$K_d^a = \frac{W}{C} \tag{5}$$

where W is the concentration of exchanged Cs^+ (mol/Kg of soil) and C is the total dissolved concentration of Cs^+ (in mol/L) which includes the concentrations of Cs^+ and CsCl(aq). The K_d^a ranges from 100 L/kg to 150 L/kg (Figure 7). These values are coherent with the K_d adopted for the calculation of the selectivity coefficient $K_{Na\text{-}Cs}$ in Equation 4.

Similar to the findings of Samper et al. (2010b), the K_d^a of Cs^+ in the DR experiment is not influenced significantly by the concentration of Cs^+ when the Cs^+ concentration is smaller than 10^{-5} mol/L because the concentration of exchanged Cs^+ is much smaller than the concentrations of other exchanged cations in the clay. The dependence of K_d^a on Cs^+ has been computed for the reference initial concentration of Cs^+ in the injection interval which is equal to $1.184 \cdot 10^{-4}$ mol/L and for a concentration ten times larger. In both cases, the K_d^a of Cs^+, decreases sharply when the concentration of dissolved Cs^+ is larger than 10^{-5} mol/L (Figure 8). Figure 8 shows also the plot of K_d^a of Cs^+ versus the ionic strength. The K_d^a of Cs^+ decreases when the ionic strength, *I*, increases because the potential competition of other cations decreases when *I* decreases. Figure 9 shows the time evolution of K_d^a and *I* at r = 0.048, 0.1, 0.5 and 1.0 m. The combined analysis of the time evolution of K_d^a and *I* illustrates clearly the inverse correlation between K_d^a and *I*. The apparent distribution coefficient, K_d^a, at r = 0.048 m increases rapidly at early times and then decreases gradually. The ionic strength shows a similar, but reversed trend. The ionic strength in the OPA pore

water decreases because the initial synthetic water has an ionic strength of 0.19 which is smaller than that of the initial OPA pore water, which is equal to 0.324 (Table 3). Away from the tracer injection interval (r > 1 m), I and K_d^a remain constant.

3.5. Uncertainty in the chemical composition of the OPA pore water

A sensitivity run was performed by assuming that the initial chemical composition of the OPA pore water is the same as the initial chemical composition of the water in the circulation system. Figure 10 shows the comparison of the radial distribution of the apparent K_d^a for the reference run, labeled as "different waters" and the sensitivity run labeled as "same waters". One can see that the space-time variability of K_d^a is large in the reference run while K_d^a remains nearly constant when the initial concentrations of the water in the circulation system and in the clay formation are identical. The variability of K_d^a in the formation from 100 to 165 L/kg is caused by the chemical gradients in the initial pore waters. Here, Ca^{2+} is also the cation that exchanges with Cs^+.

3.6. Constant K_d model

Two runs were performed with the constant K_d model for K_d = 100 and 150 L/kg, respectively. The computed results were compared with those of the MRTM. The differences between the dilution curves are very small (Figure 11). Both models fit equally well the measured data reported by Gimmi *et al.* (2014). The differences in the computed concentrations of dissolved Cs^+ in the clay formation, however, are significant (Figure 12). Therefore, the constant K_d model can be used safely to compute the concentrations in the injection interval. However, the predictions of Cs^+ migration and sorption in the rock obtained with the constant K_d model deviate from those of the MRTM. A MRTM is thus required for studying the diffusion and retention of Cs^+ in the OPA formation.

It could be claimed that a nonlinear K_d model could provide a good representation of Cs^+

diffusion and retention, but the results of the Soler et al. (2013) indicate that the nonlinear K_d model leads to biased estimates of Cs^+ sorption. The MRTM is a better representation of the real system not only because it involves more parameters than the constant K_d model, but also because it provides a more realistic mechanistic description of the coupled Cs^+ diffusion and sorption.

4. Discussion

The results of our MRTM with a single-site cation exchange are consistent with those of Jakob et al. (2009) and Soler et al. (2013) who used a 3-sites cation exchange model. They concluded that a single-species K_d model of Cs^+ is inappropriate for computing tracer profiles for laboratory and *in situ* diffusion and retention experiments. Jakob et al. (2009) reported that the competitive antagonists of Cs^+ are K^+ and Na^+ for a Cs^+ total concentration of 10^{-3} M. The results of our model indicate that Ca^{2+} is the main antagonist of Cs^+ for the DR experiment. The differences in Cs^+ antagonist cations are related to differences in the Cs^+ concentrations, the chemical composition of the OPA pore waters and the cation exchange models.

Our study shows that the sorption of Cs correlates well with the inverse of the ionic strength (Figures 8 and 9), which may change due to changes in the concentrations of dissolved species caused by solute diffusion and chemical reactions.

5. Conclusions

A multicomponent reactive transport model (MRTM) of Cs^+ for the *in situ* diffusion and retention (DR) experiment has been presented. The main conclusions of the model include:

1) Most of the solutes except for Cs^+ diffuse from the Opalinus (OPA) clay formation into the injection interval because the solute concentrations in the initial OPA clay pore water are larger than those of the initial water in the circulation system.

2) Calcite dissolves near the borehole while dolomite precipitates. Dissolved Cs^+ exchanges with Ca^{2+}.

3) The computed dilution curve of Cs^+ in the circulating fluid is sensitive to the effective diffusion, D_e, of the filter, the selectivity coefficient of Na^+ to Cs^+, and the D_e of the borehole disturbed zone.

4) The apparent distribution coefficient of Cs^+, K_d^a, in the formation varies from 100 to 165 L/kg due to the changes in the water chemistry in the formation and is inversely correlated with the ionic strength of the pore water.

5) The changes in K_d^a when the initial chemical composition of the OPA pore water is the same as the initial chemical composition of the water in the circulation system are negligible.

6) The dilution curve of Cs^+ computed with the MRTM coincides with that obtained with the K_d model. The tracer concentrations along the overcoring profiles computed with the K_d model, however, differ significantly from those computed with the MRTM.

7) A MRTM is needed for the appropriate interpretation of the Cs^+ overcoring data from the DR diffusion experiment.

The results presented in this paper could be improved by performing a thorough comparison of the computed dilution and overcoring Cs^+ concentrations with the actual data from the DR experiment reported by Gimmi *et al.* (2014). Such comparison could be performed by using the generalized 3-site cation exchange sorption model of Cs^+ of Bradbury and Baeyens (2000) and a dual porosity MRTM such as that reported by Appelo et al. (2010).

Acknowledgements. This work was supported by ENRESA, the European Union through the FUNMIG (FUNdamental Processes of radionuclide MIGration) Project (FP6-516514), the

Mont Terri Consortium and a research scholarship awarded to the third author. Funding for the latest stages of the work was provided by the Spanish Ministry of Economy and Competitiveness (Project CGL2012-36560), and Fund 2012/181 from "*Consolidación e estruturación de unidades de investigación competitivas", Grupos de referencia competitiva"*) of Xunta de Galicia. Partial funding has been obtained from the National Natural Science Foundation of China through 41202163 and the Guangdong Natural Science Foundation through S2011040005245. Thanks are given to Olivier Leupin from NAGRA and Thomas Gimmi from PSI and the University of Bern for productive discussions on the DR experiments. We thank the four anonymous reviewers for their constructive and thoughtful comments and suggestions, which have contributed to improve the paper.

References

Appelo, C. A. J., and Postma, D., 1993, Geochemistry, groundwater and pollution, Balkema, Rotterdam, 536 pp.

Appelo, CAJ, Van Loon, LR, Wersin, P., (2010). Multicomponent diffusion of a suite of tracers (HTO, Cl, Br, I, Na, Sr, Cs) in a single simple of Opalinus Clay. Geochimica et Cosmochimica Acta 74, 1201-1219

Atun, G. and Bodur, N., (2002). Retention of Cs on zeolite, bentonite and their mixtures. Journal of Radioanalytical and Nuclear Chemistry, 253 (2), 275-279.

Atun, G. and Kilislioglu, A., (2003). Adsorption behavior of cesium on montmorillonite-type clay in the presence of potassium ions. Journal of Radioanalytical and Nuclear Chemistry, 258 (3), 605-611.

Bradbury, M.H., Baeyens, B., (2000). A generalised sorption model for the concentration dependent uptake of caesium by argillaceous rocks. J. Contam. Hydrol. 42, 141–163.

Dai, Z.; Samper, J.; Ritzi, R., 2006. Identifying geochemical processes by inverse modeling of multicomponent reactive transport in Aquia aquifer. Geosphere, 4, 210–219.

Dai, Z.; Samper, J., 2006. Inverse modeling of water flow and multicomponent reactive transport in coastal aquifer systems. Journal of Hydrology, 327, 447-461.

Dai, Z., A. Wolfsberg, Z. Lu, and H. Deng, (2009) Scale dependence of sorption coefficients for contaminant transport in saturated fractured rock, Geophysical Research Letters, 36, L01403, doi:10.1029/2008GL036516, 2009.

Dai, Z., A. Wolfsberg, P. Reimus, H. Deng, E. Kwicklis, M. Ding, D. Ware and M. Ye, (2012) Identification of

sorption processes and parameters for radionuclide transport in fractured rock, J. of Hydrol., v 414-415, 516-526.

Dewonck, S. (2007). Expérimentation DIR. Synthese des résultats obtenus au 01/03/07. Laboratoire de recherche souterrain de Meuse/Haute-Marne. ANDRA report D.RP.ALS.07-0044.

Gaines, L.G.; Thomas, C.H., 1953. Adsorption studies on clay minerals. II. A formulation of the thermodynamics of exchange adsorption. J. Chem. Phys. 21, 714–718.

García-Gutiérrez, M., Missana, T., Mingarro, M., Samper, J., Dai, Z., Molinero, J., (2001). Solute transport properties of compacted Ca-bentonite used in FEBEX Project. J. Contam. Hydrol. 47 (3), 127–137.

Gimmi, T., 2006. DR experiment Mont Terri: Compilation of input data for calculations. Technical Note of the DR Project.

Gimmi, T., 2009. DR_SampleData_25Jun09. Technical Documentation of the DR Project.

Gimmi T, O Leupin, J Eikenberg, M Glaus, L R. Van Loon, N Waber, P Wersin, H Wang, D Grolimund, C N. Borca, S Dewonck, C Wittebrood, 2014, Anisotropic diffusion at the field scale in a 4-year multi-tracer diffusion and retention experiment – I: Insights from the experimental data, Geochimica et Cosmochimica Acta 125 (2014) 373–393. http://dx.doi.org/10.1016/j.gca.2013.10.014.

Gutiérrez; M. and Fuentes, H.R.,(1996) A mechanistic modeling of montmorillonite contamination by cesium sorption. Applied Clay Science, 11, 11-24.

Jakob A., Pfingstein W., and Van Loon, L., (2009). Effects of sorption competition on caesium diffusion through compacted argillaceous rock. Geochimica et Cosmochimica Acta, 73, 2441-2456.

Jan, Y.L., Tsai, S.C., Jan, J.C. and Hsu, C.N., 2006. Additivity of the distribution ratio of Cs and Se on bentonite/quartz sand mixture in seawater. Journal of Radioanalytical and Nuclear Chemistry, 267 (1), 225-231.

Khan, S.A., 2003. Sorption of the long-lived radionuclides cesium-134, strotium-85 and cobalt-60 on bentonite. Journal of Radioanalytical and Nuclear Chemistry, 258 (1), 3-6.

Klika, Z., Kraus, L. and Vopalka, D., (2007). Cesium Uptake from Aqueous Solutions by Bentonite: A Comparison of Multicomponent Sorption with Ion-Exchange Models. Langmuir 23, 1227-1233.

Lauber, M., Baeyens, B., Bradbury, M.H., (2000). Physico-chemical characterization and sorption measurements of Cs, Sr, ni, Eu, Th, Sn and Se on Opalinus Clay from Mont Terri. PSI Technical Report 00-10. Also in: Nagra Tecnnical Report NTB 00-11.

Lu, C, J Samper, B. Fritz, A. Clement & L. Montenegro, 2011, Interactions of corrosion products and bentonite: An extended multicomponent reactive transport model, Physics and Chemistry of the Earth, Parts A/B/C, Vol 36:1661–1668 doi:10.1016/j.pce.2011.07.013

Molinero, J.; Samper, J.; Yang, C.; Zhang, G., 2004. Biogeochemical reactive transport model of the Redox zone experiment of the Äspö hard rock laboratory (Sweden). Nuclear Technology, 48(2), 151-165.

Molinero, J.; Samper, J., 2006. Modeling of reactive solute transport in fracture zones of granitic bedrocks. Journal of Contaminant Hydrology, 82, 293–318.

Montavon, G., Alhajji, E. and Grambow, B., (2006). Study of the interaction of Ni^{2+} and Cs^{+} on MX-80 bentonite: effect of compaction using the "Capillary method". Environmental Science and Technology, 40, 4672-4679.

Murali, M.S. and Mathur, J.N., (2002). Sorption characteristics of Am(III), Sr(II) and Cs(I) on bentonite and granite. Journal of Radioanalytical and Nuclear Chemistry, 254(1), 129-136.

Naves, A, J Samper & T Gimmi, 2012, Identifiability of diffusion and sorption parameters from *in situ* diffusion experiments by using simultaneously tracer dilution and claystone data, Journal of Contaminant Hydrology 142-143 (2012) 63–74. http://dx.doi.org/10.1016/j.jconhyd.2012.09.005.

Palut, J.M., Montarnal, P., Gautschi, A., Tevissen, E., Mouche, E., 2003. Characterisation of HTO diffusion properties by an *In situ* tracer experiment in Opalinus Clay at Mont Terri. Journal of Contaminant Hydrology, 61(1), 203-218.

Pearson, F.J., Arcos, D., BOISSON, J.-Y., Fernandes, A.M., Gabler, H.-E., Gaucher, É., Gautschi, A., Griffault, L., Hernan, P., Waber, H.N., 2003. Geochemistry of Water in the Opalinus Clay Formation at the Mont Terri Rock Laboratory. Federal Office for Water and Geology. Geology Series, vol. 5.

Shahwan, T. and Erten, H.N., (2002). Thermodynamic parameters of Cs^{+} sorption on natural clays. Journal of Radioanalytical and Nuclear Chemistry, 253 (1), 115-120.

Samper, J., Yang, C.B., Montenegro, L., 2003. Users Manual of CORE2D version 4: A Code for groundwater flow and Reactive solute transport. Technical Report, UDC, 83 pp.

Samper, J., Yang, C., Naves, A., Yllera, A., Hernández, A., Molinero, J., Soler, J.M., Hernán, P., Mayor, J.C., Astudillo, J., (2006a) A fully 3-D anisotropic model of DI-B *in situ* diffusion experiment in the Opalinus Clay formation. Physics and Chemistry of the Earth, 31, 531-540.

Samper, J., Dai, Z., Molinero, J., García-Gutiérrez, M., Missana, T., Mingarro, M., (2006b). Interpretation of solute transport experiments in compacted Ca-bentonites using inverse modelling. Physics and Chemistry of the Earth 31, 640-648.

Samper, J., Yang, C., 2006. Stochastic Analysis of Transport and Multicomponent Competitive Monovalent Cation Exchange in Aquifers. Geosphere, April, 2, 102-112.

Samper, J., Dewonck, S., Zheng, L., Yang, Q., Naves, A., (2008a). Normalized sensitivities and parameter identifiability of *in situ* diffusion experiments on Callovo-Oxfordian clay at Bure site. Physics and Chemistry of the Earth, 33, 1000-1008.

Samper, J., C. Lu, & L. Montenegro, (2008b) Coupled hydrogeochemical calculations of the interactions of corrosion products and bentonite, Physics and Chemistry of the Earth, Vol. 33. Supplement 1, S306-S316.

Samper, J., T. Xu and C. Yang, 2009, A sequential partly iterative approach for multicomponent reactive transport with CORE^{2D}, Comput Geosci DOI 10.1007/s10596-008-9119-5.

Samper, J, S. Yi, A. Naves, 2010a. Analysis of the parameter identifiability of the *in situ* diffusion and retention （DR） experiment. Physics and Chemistry of the Earth, 35, 207-216.

Samper J, C Lu, JL Cormenzana, H Ma, L Montenegro & MA Cuñado, 2010b, Testing Kd models of Cs+ in the near field of a HLW repository in granite with a reactive transport model, Physics and Chemistry of the Earth, Vol 35:278–283 doi:10.1016/j.pce.2010.04.002.

Samper, J, C Yang, L. Zheng, L. Montenegro, T Xu, Z Dai, G Zhang, C Lu & S Moreira, (2011), CORE^{2D} V4: A code for water flow, heat and solute transport, geochemical reactions, and microbial processes, Chapter 7 of the Electronic book Groundwater Reactive Transport Models, F Zhang, G-T Yeh, C Parker & X Shi (Ed), Bentham Science Publishers, pp 161-186.

Soler J.M, J. Samper, A. Yllera, A. Hernández, A. Quejido, M. Fernández, C. Yang, A. Naves, P. Hernán, and P. Wersin, (2008) The DI-B in-situ diffusion experiment at mont terri: results and modelling, Physics and Chemistry of the Earth, Vol. 33. Supplement 1, 2008, S196-S207.

Soler, JM, P Wersin, O X. Leupin, (2013) Modeling of Cs^+ diffusion and retention in the DI-A2 experiment (Mont Terri). Uncertainties in sorption and diffusion parameters, Applied Geochemistry 33 (2013) 191–198.

Tertre, E., Berger, G., Castel, S., Loubet, M. and Giffaut, E., (2005). Experimental sorption of Ni^{2+}, Cs^+ and Ln^{3+} onto a montmorillonite up to 150°C. Geochimica et Cosmochimica Acta, 69(21), 4937-4948.

Tevissen, E., Soler, J. M., Montarnal, P., Gautschi, A., van Loon, L.R., (2004). Comparison between *in situ* and laboratory diffusion studies of HTO and halides in Opalinus Clay from the Mont Terri. Radiochimica Acta, 92, 781-786.

Tsai, S.C., Ouyang, S. and Hsu, C.N., (2001) Sorption and diffusion behaviour of Cs and Sr on Jih-Hsing bentonite. Applied Radiation and Isotopes, 54, 209-215.

Van Loon, L.R., Glaus, M.A., (2008). Effective diffusion coefficient of several tracers in Teflon filters. PSI Technical note, Switzerland.

Van Loon L. R., Wersin P., Soler J. M., Eikenberg J., Gimmi T., Hernán P., Dewonck S., Savoye S. (2004). In-Situ Diffusion of HTO, $^{22}Na^+$, Cs^+ and I^- in Opalinus Clay at the Mont Terri Underground Rock Laboratory. Radiochimica Acta, 92, 757-763.

Van Loon, L.R., Baeyens, B., Bradbury M.H., (2009). The sorption behaviour of caesium on Opalinus Clay: A

comparison between intact and crushed material, Applied Geochemistry, doi: 10.1016/j.apgeochem.2009.03.003.

Wersin, P., Van Loon, L. R., Soler, J., Yllera, A., Eikenberg, J., Gimmi, T., Hernan, P., Boisson, J.-Y., (2004). Long-term Diffusion Experiment at Mont Terri: First Results from Field and Laboratory Data. Applied Clay Science, 26, 123-135.

Wersin, P., Soler, J.M., Van Loon, L., Eikenberg, J., Baeyens, B., Grolimund, D., Gimmi, T., Dewonck, S., (2008). Diffusion of HTO, Br^-, I^-, Cs^+, $^{85}Sr^{2+}$ and $^{60}Co^{2+}$ in a Clay Formation: Results and Modelling from an *in situ* Experiment in Opalinus Clay. Applied Geochemistry 23 (4), 678-691.

Wolery, T.J., 1992. EQ3/6, a software package for geochemical modeling of aqueous systems: Package overview and installation guide. Lawrence Livermore National Laboratory. Livermore. California. Version: thermo.com.8, 230.

Xu, T., Samper, J., Ayora, C., Mazano, M. and Custodio, E., 1999. Modeling of nonisothermal multi-component reactive transport in field-scale porous media flow system. Journal of Hydrology, 214, 144-164.

Yang, C., Samper, J., Molinero J., Bonilla M., 2007. Modelling geochemical and microbial consumption of dissolved oxygen after backfilling a high level radioactive waste repository, J Cont Hydrol, 93 130–148

Yang, C., J. Samper, & L. Montenegro, 2008, A coupled non-isothermal reactive transport model for long-term geochemical evolution of a HLW repository in clay, Environmental Geology, 53, 1627–1638. DOI 10.1007/s00254-007-0770-2.

Yeh, G.T., 2000. Computational subsurface hydrology reactions, transport, and fate of chemicals and microbes. Kluwer, Dordrecht.

Yi, S, J Samper, A Naves, & J M. Soler, 2012, Inverse Estimation of the Effective Diffusion of the Filter in the *In situ* Diffusion and Retention (DR) Experiment, Transport in Porous Media, DOI 10.1007/s11242-012-9960-9

Yllera A., Hernández A., Mingarro M., Quejido A., Sedano L. A., Soler J. M., Samper J., Molinero J., Barcala J. M., Martín P. L., Fernández M., Wersin P., Rivas P. & Hernán P. (2004) DI-B Experiment: Planning, Design and Performance of an *In situ* Diffusion Experiment in the Opalinus Clay Formation. Applied Clay Science 26, 181-196.

Zhang G, J. Samper & L. Montenegro (2008) Coupled thermo-hydro-bio-geochemical reactive transport model of the CERBERUS heating and radiation experiment in Boom clay, Appl Geochem, Vol 23/4: 932-949.

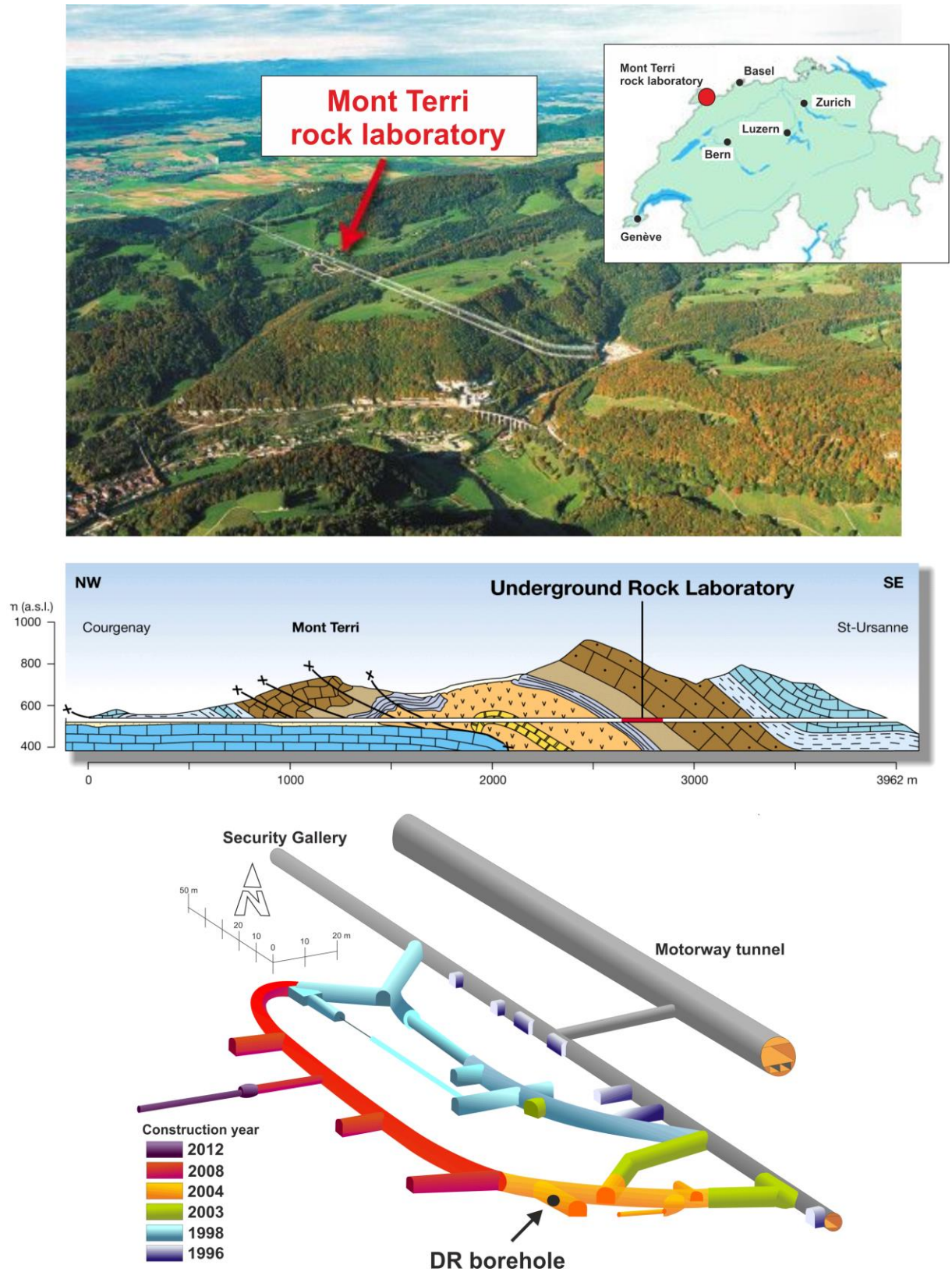

Figure 1. *Location of the Mont Terri underground research laboratory (top) and situation of the DR borehole (modified from www.mont-terri.ch)*

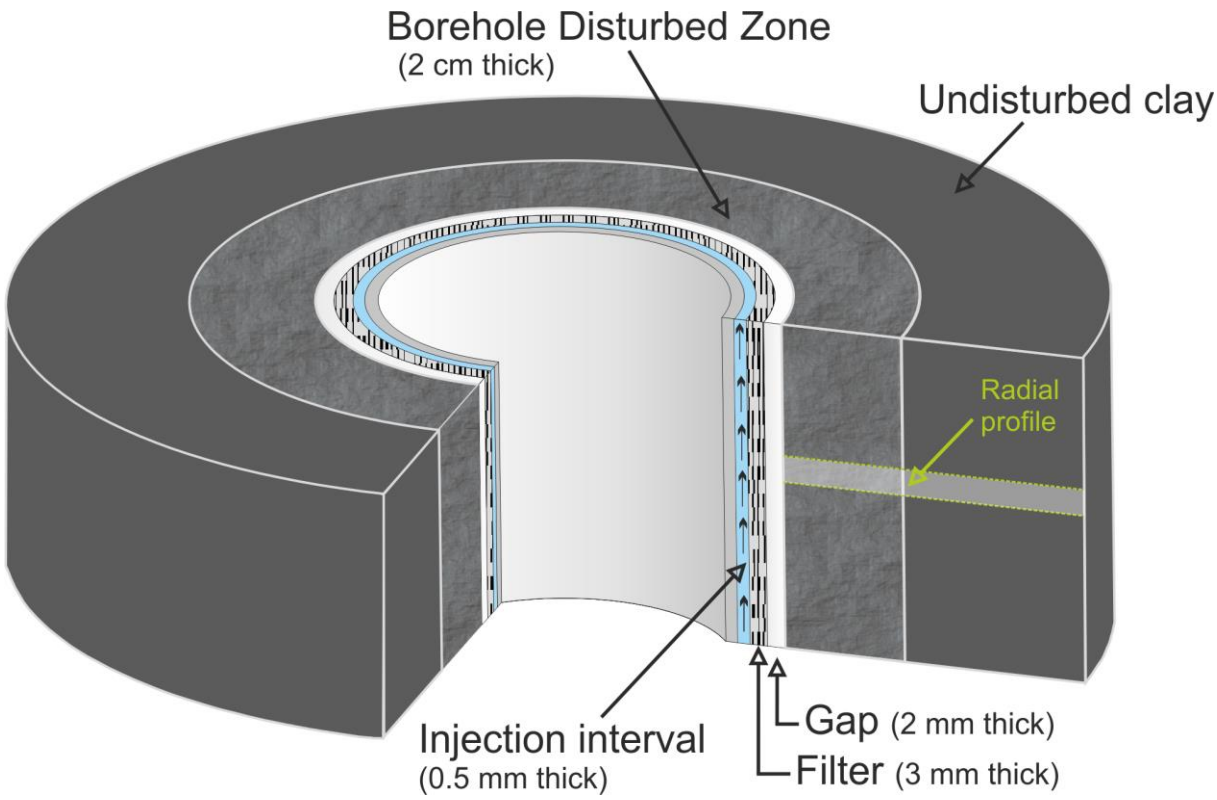

Figure 2. *Sketch of the borehole geometry for the DR experiment (modified from Samper et al. 2008a).*

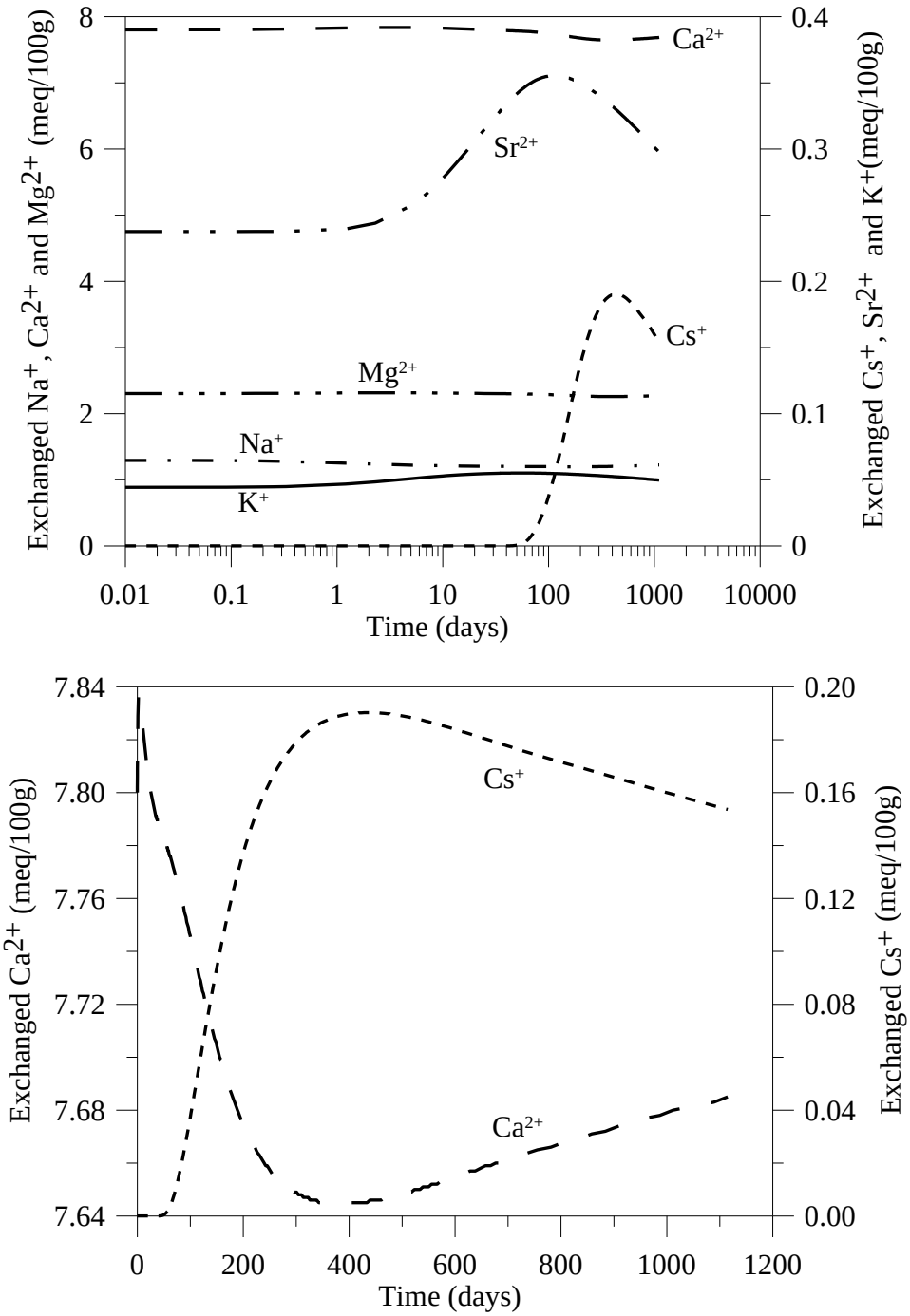

Figure 3. *Time evolution of the computed concentrations of exchanged cations at r = 0.048 m (top plot). The bottom plot shows a zoom of the time evolution of the computed concentrations of exchanged Ca^{2+} and Cs^{+}.*

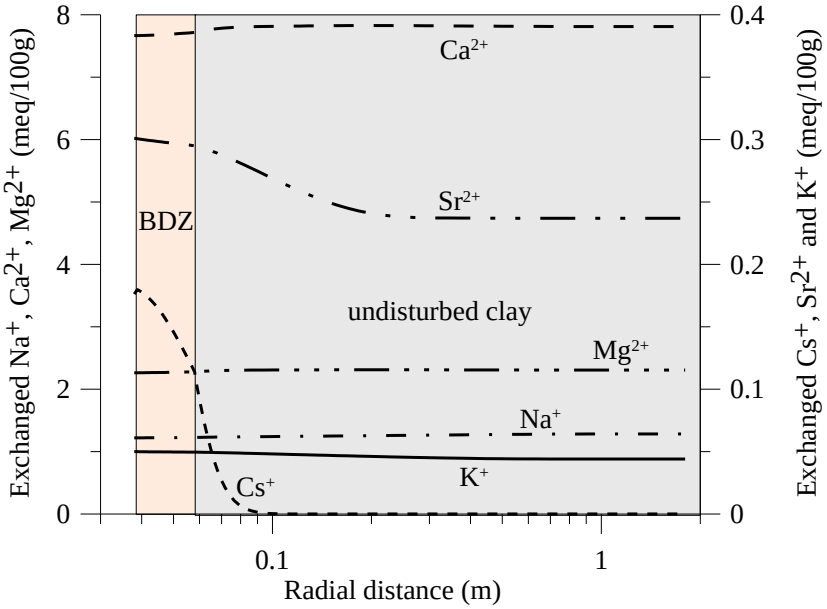

Figure 4. *Radial distribution of the computed concentrations of the exchanged cations at t = 1115 days.*

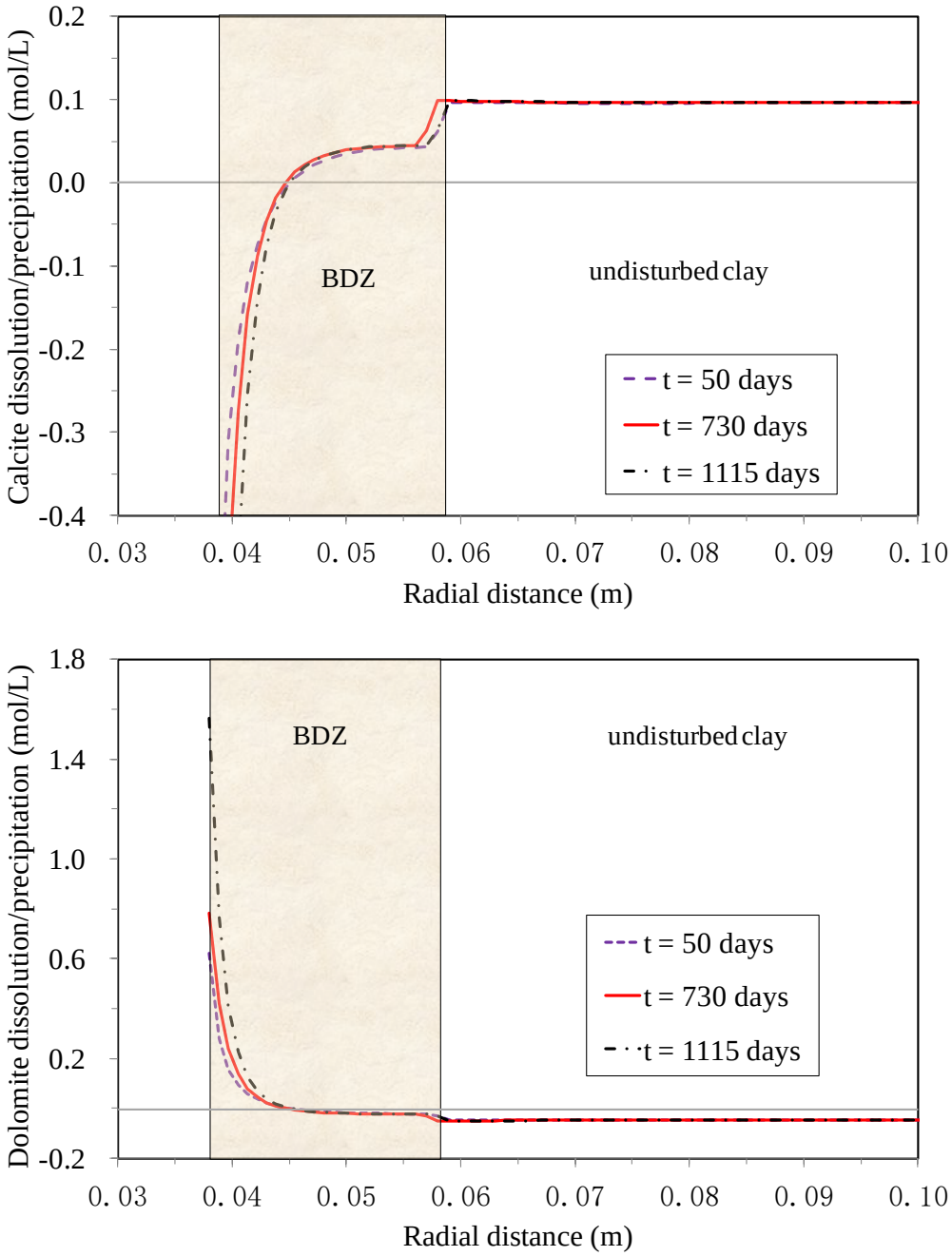

Figure 5. *Radial distribution of the computed cumulative concentration of dissolved/precipitated calcite (top plot) and dolomite (bottom plot) at selected times (negative values correspond to dissolution and positive values for precipitation).*

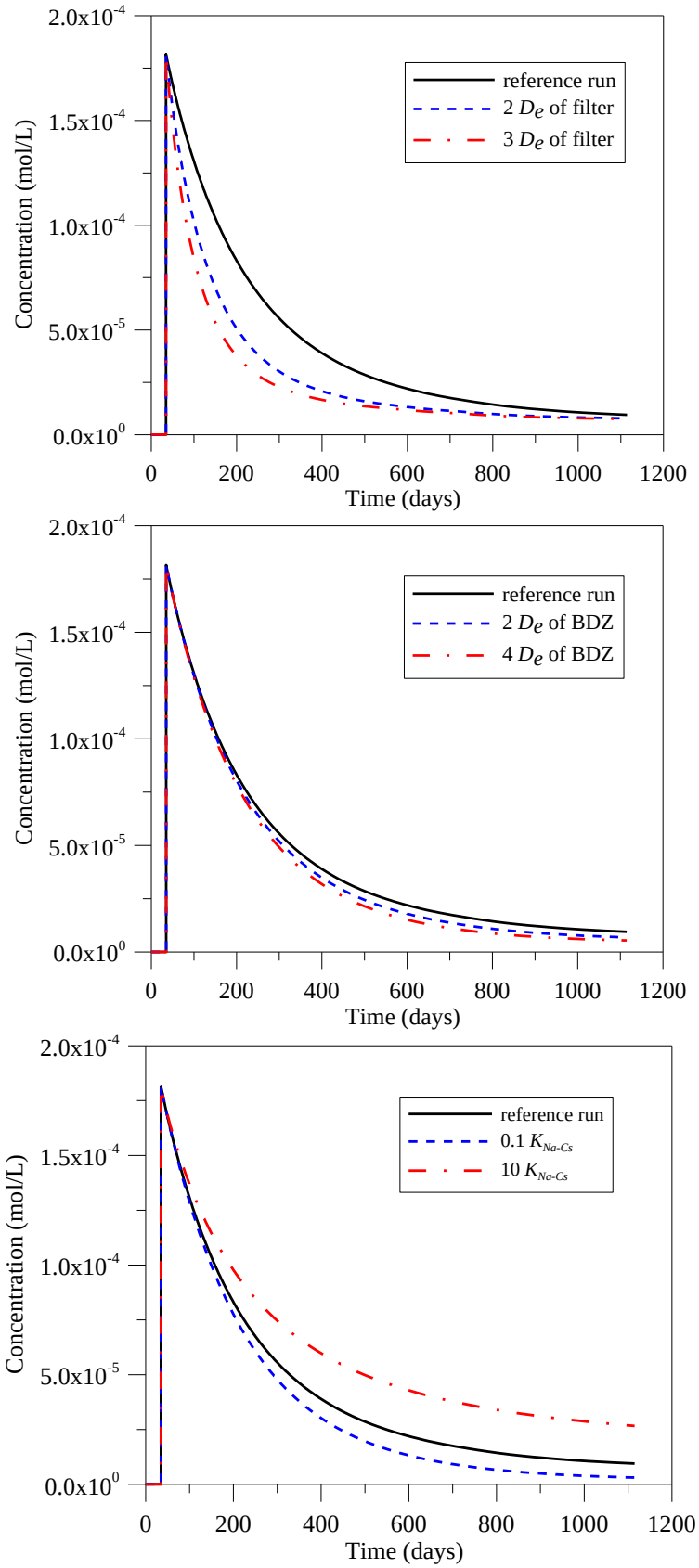

Figure 6. *Sensitivity of the dilution curves of Cs^+ at the injection interval to changes in the effective diffusion of the filter (top plot), the effective diffusion of the BDZ (intermediate plot) and the selectivity coefficient $K_{Na\text{-}Cs}$ (bottom plot).*

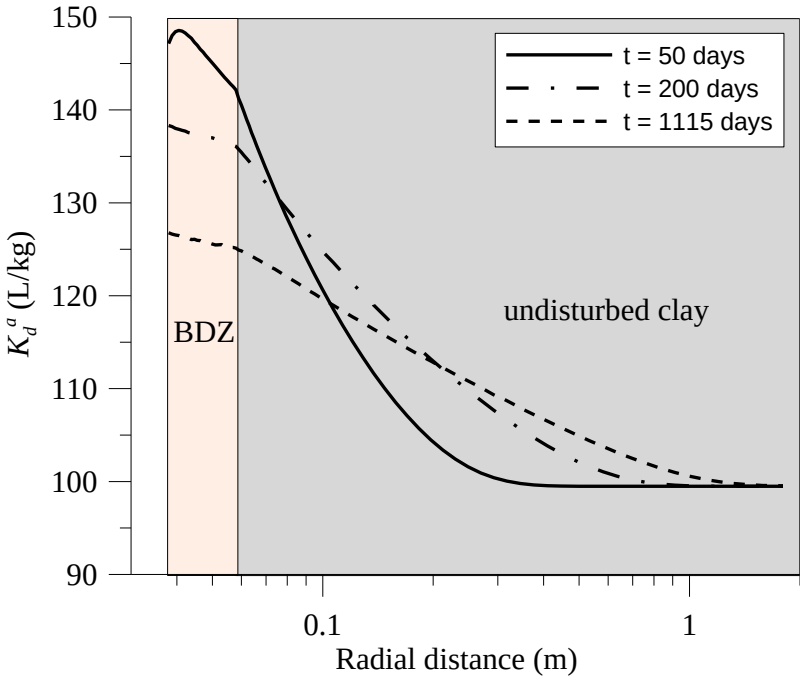

Figure 7. *Radial distribution of the computed apparent distribution coefficient, K_d^a, of Cs^+ at selected times.*

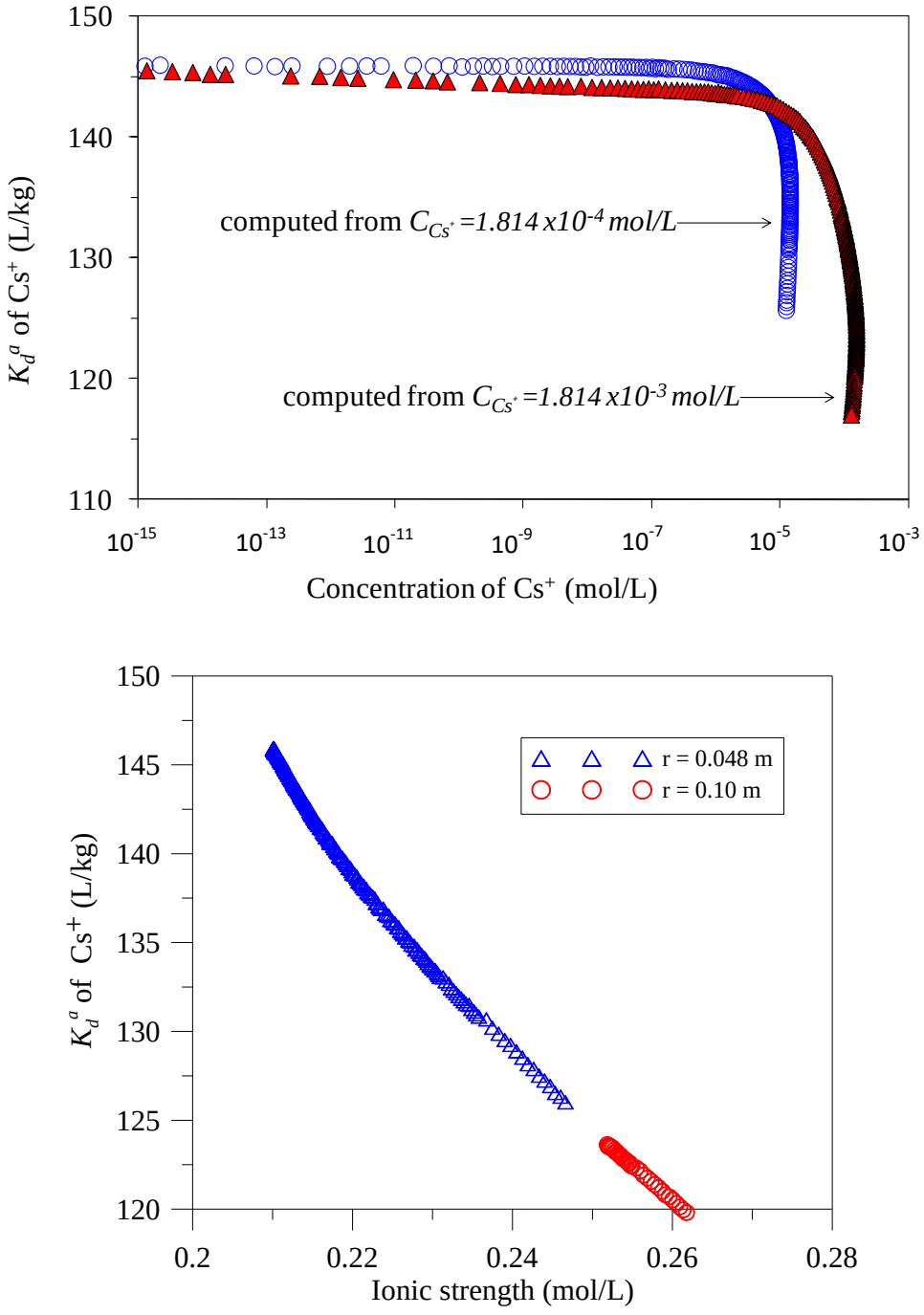

Figure 8. *Computed apparent distribution coefficient,* K_d^a , of Cs^+ *versus* log-*concentration of* Cs^+ *at r = 0.048 m (top plot) and versus the ionic strength at r = 0.048 and 0.1 m (bottom plot).*

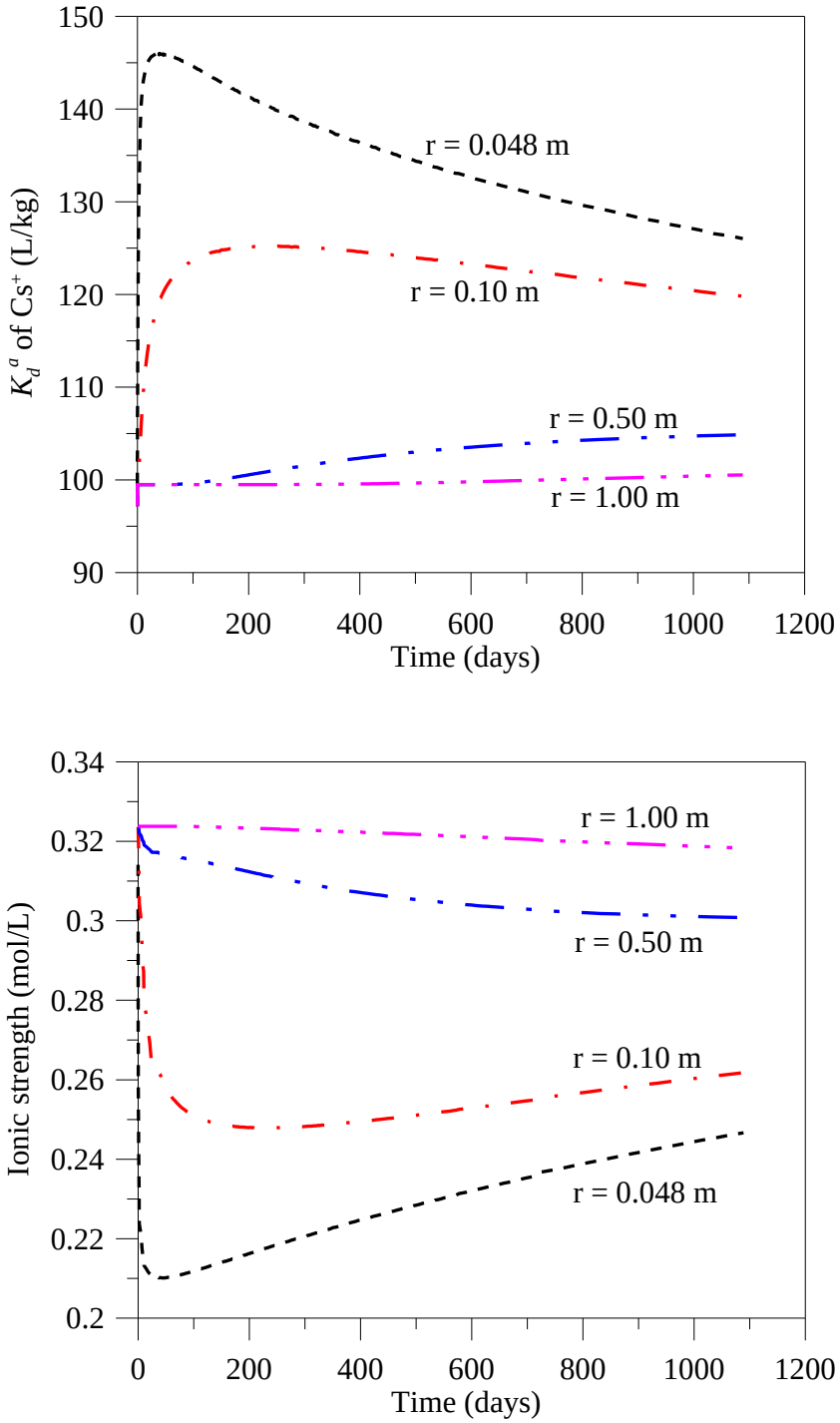

Figure 9. *Computed time evolution of the apparent distribution coefficient,* K_d^a *of* Cs^+ *(top) and ionic strength (bottom) at r = 0.048, 0.068, 0.1, 0.5 and 1.0 m.*

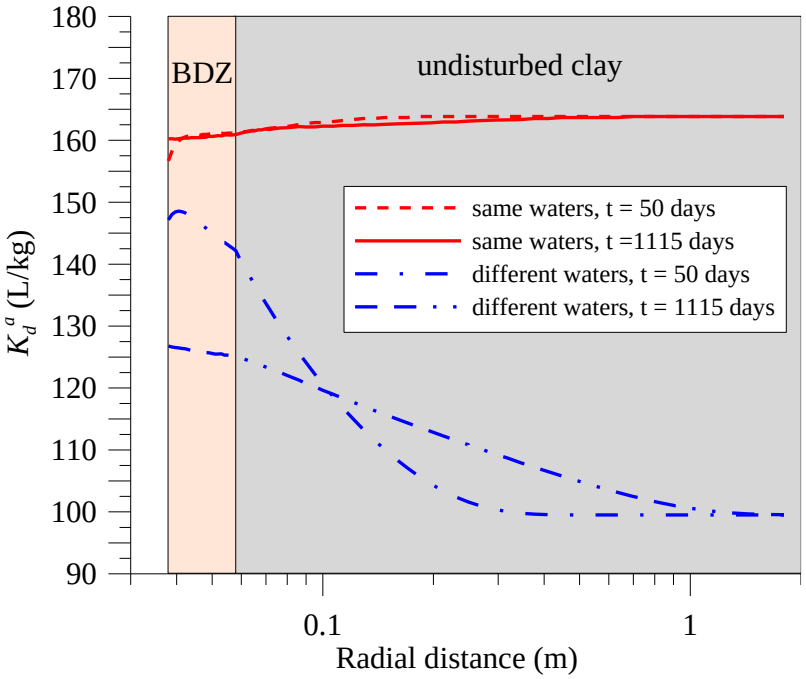

Figure 10. *Radial distribution of apparent distribution coefficient, K_d^a of Cs^+ at t = 50 and 1115 days for the reference run (labeled as "different waters") and the sensitivity run (labeled as "same waters") in which the initial chemical composition of the clay pore water is the same as the initial chemical composition of the water in the circulation system.*

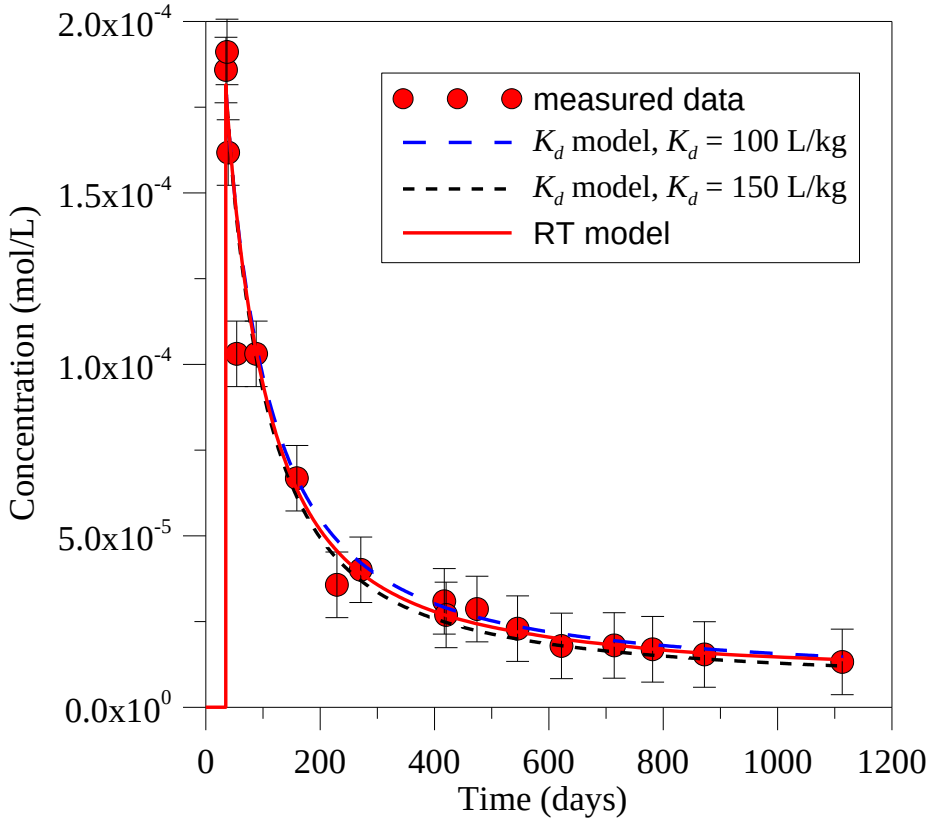

Figure 11. *Comparison of the dilution curves of Cs^+ computed with the MRTM and the constant K_d model with K_d = 100 and 150 L/kg. The plot shows also the measured data (symbols) reported by Gimmi et al. (2014).*

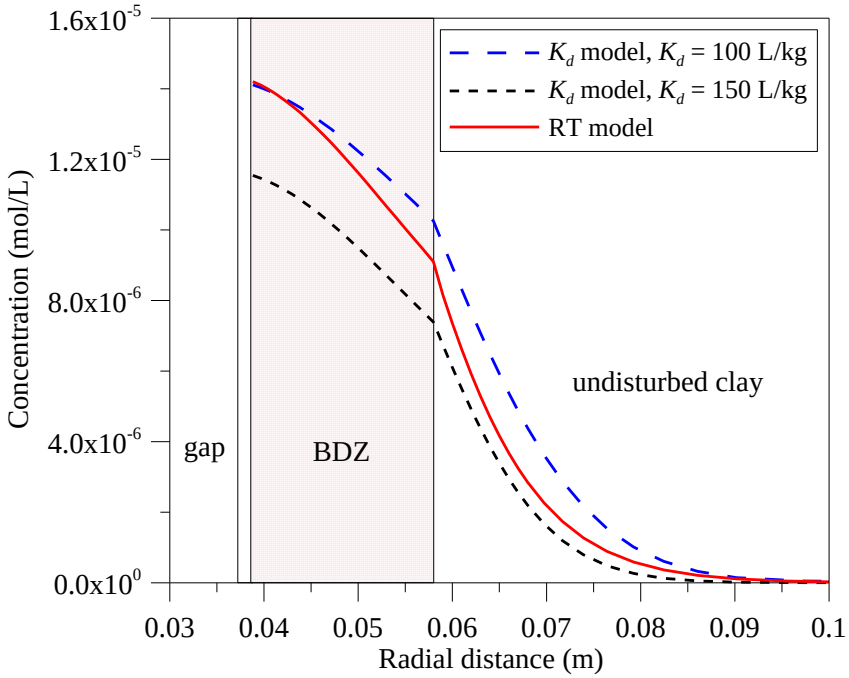

Figure 12. *Radial distribution of the Cs^+ concentrations computed with the MRTM and the constant K_d model with K_d = 100 and 150 L/kg.*

Table 1. *Effective diffusion, D_e, and porosity, Φ for the filter, the gap, the BDZ and the undisturbed clay. The parameters of the undisturbed clay were derived from Gimmi (2006). The D_e of the gap and the BDZ were computed from those of the undisturbed clay by using Archie´s law with an exponent of 1.33. The D_e of the filter was measured by van Loon and Glaus (2008) and is equal to 10% of the value in free water.*

Filter		Gap		BDZ		Undisturbed clay	
D_e (10^{-10} m^2/s)	Φ (-)	D_e (10^{-10} m^2/s)	Φ (-)	D_e (10^{-10} m^2/s)	Φ (-)	D_e (10^{-10} m^2/s)	Φ (-)
3.76	0.3	19.0	0.6	7.56	0.3	3.0	0.15

Table 2. *Chemical reactions and equilibrium constants at 25℃ for aqueous complexes, minerals and cation exchange reactions. The log K values of aqueous complexes and minerals were taken from Wolery (1992). The selectivity coefficients for cation exchange reactions were taken from Pearson et al. (2003) except for the selectivity coefficient of Cs^+ to Na^+ which was estimated from Equation 4.*

Aqueous complexes	**Log *K***
$CaSO_4(aq) \Leftrightarrow Ca^{2+} + SO_4^{2-}$	-2.1111
$CaCl^+ \Leftrightarrow Ca^{2+} + Cl^-$	0.6956
$CaHCO_3^+ \Leftrightarrow Ca^{2+} + HCO_3^-$	-1.0467
$CaCO_3(aq) \Leftrightarrow Ca^{2+} + CO_3^{2-}$	7.0017
$CaCl_2(aq) \Leftrightarrow Ca^{2+} + 2Cl^-$	0.6436
$NaHCO_3(aq) \Leftrightarrow Na^+ + HCO_3^-$	-0.1541
$CO_2(aq) + H_2O \Leftrightarrow H^+ + HCO3^-$	-6.3447
$MgCO_3(aq) + H^+ \Leftrightarrow Mg^{2+} + HCO_3^-$	7.3499
$CO_3^{2-} + H^+ \Leftrightarrow HCO3^-$	10.329
$NaCO_3^- + H^+ \Leftrightarrow Na^+ + HCO_3^-$	9.8144
$KSO_4^- \Leftrightarrow K^+ + SO_4^{2-}$	-0.8796
$KCl(aq) \Leftrightarrow K^+ + Cl^-$	1.4946
$MgSO_4(aq) \Leftrightarrow Mg^{2+} + SO_4^{2-}$	-2.4117
$MgCl^+ \Leftrightarrow Mg^{2+} + Cl^-$	0.1349
$MgHCO_3^+ \Leftrightarrow Mg^{2+} + HCO_3^-$	-1.0357
$NaCl(aq) \Leftrightarrow Na^+ + Cl^-$	-0.777
$NaSO_4^- \Leftrightarrow Na^+ + SO_4^{2-}$	-0.82
$SrSO_4(aq) \Leftrightarrow Sr^{2+} + SO_4^{2-}$	-2.3
$SrCl^+ \Leftrightarrow Sr^{2+} + Cl^-$	0.2485
$SrCO_3(aq) + H^+ \Leftrightarrow Sr^{2+} + HCO_3^-$	7.4635
$OH^- + H^+ \Leftrightarrow H_2O$	13.995
$CsCl(aq) \Leftrightarrow Cs^+ + Cl^-$	0.1385
Minerals	**Log *K***
$CaCO_3(s) + H^+ \Leftrightarrow Ca^{2+} + HCO_3^-$	1.8487
$CaMg(CO_3)_2(s) + 2H^+ \Leftrightarrow Mg^{2+} + Ca^{2+} + 2HCO_3^-$	3.5676
$CaSO_4 \cdot 2H_2O(s) \Leftrightarrow Ca^{2+} + SO_4^{2-} + 2H_2O$	-4.4823
Exchanged cations	$K_{\text{Na-cation}}$
$Na^+ + X\text{-}K \Leftrightarrow K^+ + X\text{-}Na$	0.1995
$Na^+ + 0.5X_2\text{-}Ca \Leftrightarrow 0.5Ca^{2+} + X\text{-}Na$	0.0792
$Na^+ + 0.5X_2\text{-}Mg \Leftrightarrow 0.5Mg^{2+} + X\text{-}Na$	0.1256
$Na^+ + 0.5X_2\text{-}Sr \Leftrightarrow 0.5Sr^{2+} + X\text{-}Na$	0.0615
$Na^+ + X\text{-}Cs \Leftrightarrow Cs^+ + X\text{-}Na$	$4.76 \cdot 10^{-4}$

Table 3. *Chemical composition of the synthetic water in the circulation system (Gimmi et al. 2014), the initial OPA pore water taken from van Loon et al. (2009) and the initial OPA pore water after equilibration with calcite and dolomite.*

	Synthetic water in the circulation system (mol/ L)	Initial OPA pore water (mol/ L)	Initial OPA pore water after equilibration with calcite and dolomite (mol/ L)
pH	7.38	7.60	7.22
Cl^-	$1.80\cdot10^{-1}$	$3.00\cdot10^{-1}$	$3.00\cdot10^{-1}$
HCO_3^-	$2.97\cdot10^{-3}$	$4.76\cdot10^{-4}$	$4.41\cdot10^{-4}$
SO_4^{2-}	$9.16\cdot10^{-3}$	$1.40\cdot10^{-2}$	$1.41\cdot10^{-2}$
Na^+	$1.43\cdot10^{-1}$	$2.40\cdot10^{-1}$	$2.37\cdot10^{-1}$
Ca^{2+}	$8.40\cdot10^{-3}$	$2.60\cdot10^{-2}$	$2.25\cdot10^{-2}$
Mg^{2+}	$1.08\cdot10^{-2}$	$1.70\cdot10^{-2}$	$2.13\cdot10^{-2}$
K^+	$1.43\cdot10^{-3}$	$1.60\cdot10^{-3}$	$1.57\cdot10^{-3}$
Sr^{2+}	$4.68\cdot10^{-4}$	$5.10\cdot10^{-4}$	$4.78\cdot10^{-4}$
Ionic strength	$1.90\cdot10^{-1}$	$3.24\cdot10^{-1}$	$3.24\cdot10^{-1}$

Table 4. *Computed charge balance errors at the end of simulation at selected radial distances.*

Radial distance (m)	Positive Charge |PC|	Negative Charge |NC|	Charge Error CE = |PC-NC|	Mean charge MC = (PC+NC)/2	Relative Error CE/MC×100 (%)
0.048	0.2203	0.2290	0.0087	0.2247	3.9
0.1	0.2351	0.2419	0.0068	0.2385	2.9
0.5	0.2746	0.2765	0.0019	0.2756	0.7
1	0.2879	0.2882	0.0003	0.2881	0.1